

XRISM: X-ray imaging and spectroscopy mission

Makoto S. Tashiro

The Institute of Space and Astronautical Science, JAXA

Tsukuba, Ibaraki, Kanagawa, 305-8505, Japan

Department of Physics, Saitama University

Sakura-ku, Saitama, Saitama, 338-8570, Japan

tashiro@mail.saitama-u.ac.jp

and the XRISM team

The X-Ray Imaging and Spectroscopy Mission (XRISM) is a JAXA/NASA X-ray observatory with collaboration from ESA and several institutes and academic institutions worldwide. It is proposed to fulfill the promise of high-resolution X-ray spectroscopy with imaging once realized but unexpectedly terminated by a mishap of ASTRO-H/Hitomi. XRISM carries two sets of X-ray Mirror Assemblies and is equipped on the focal plane with a 6×6 pixelized X-ray micro-calorimeter array and an aligned X-ray CCD camera. With the combination of high-resolution spectroscopy imaging and the broader field of view, XRISM is expected to pioneer a new horizon of the Universe in X-ray astrophysics. Aiming to launch the satellite in the Japanese Fiscal Year 2022, we fabricate the instruments and test for the satellite integration starting at the beginning of 2022. The paper reports the development status, reviewing the science objectives and the operation plan.

Keywords: X-ray astronomy; observation satellite; spectroscopy; imaging

1. Overview of XRISM

The X-ray imaging and spectroscopy mission — XRISM^{1,2} is a recovery mission of ASTRO-H Hitomi³ launched on February 17, 2016. After the launch and following the commissioning of the onboard instruments, Hitomi started observation. However, due to a series of mishaps in the attitude control system, Hitomi was forced to stop operation on March 26. The observation period was only one month, but the results clearly show the X-ray microcalorimeter epoch-making capability. The observation was terminated before opening the gate valve. The valve was equipped to protect the sensor assembly from the atmosphere on the ground, but the gate valve limited the bandpass below ~ 2 keV. Even with the limitation in the low energy band, the unprecedented energy resolution enables us to measure the plasma turbulence velocity and detect weak lines of rare metals with a few ks exposure. The obtained spectrum is a highlight obtained from the Perseus cluster of galaxies.⁴

The central concept of XRISM is to maximize the X-ray micro-calorimeter science since it is an entirely new scientific field. We chose a conservative combination

with the CCD camera to strengthen the science. Table 1 summarizes of required specifications of the instruments of XRISM.

Table 1. XRISM mission instruments specifications

Parameters	Resolve	Xtend
Feild of view	$\geq 2.9' \times 2.9'$	$\geq 22' \times 22'$
Angular resolution [†]	$\leq 1.7'$	$\leq 1.7'$
Effective area at 6 keV	$\geq 210 \text{ cm}^2$	$\geq 300 \text{ cm}^2$
Imaging pixel format	6×6	1280×1280
Energy range	0.3 – 12 keV	0.4 – 13 keV
Energy resolution [‡]	$\leq 7 \text{ eV}$ (goal 5 eV)	$\leq 250 \text{ eV}^*$

[†]: The half power diameter

[‡]: The full width half maximum at 6 keV

*: At the end of mission life.

1.1. *Resolve*

The critical device of XRISM — the X-ray microcalorimeter realizes the high-resolution spectroscopy with imaging by the X-ray Mirror Assembly (XMA). The XMA is a Wolter-I X-ray mirror of their reflectors' figure in conical approximation. The reflectors of the mirror are made of heat formed aluminum substrate followed by epoxy replication on gold-sputtered smooth Pyrex cylindrical mandrels. The XMA is developed and fabricated by NASA/Goddard Space Flight Center (GSFC). The imaging spectroscopy telescope of XRISM is named “Resolve.”⁵ The device measures phonons induced by a penetrated X-ray photon. The X-ray photon heats the mercury tellurized absorber by a few mK, and the temperature rise is measured by the attached silicon thermometer in the accuracy of μK . All the pixelized detectors are cooled down to 50 mK to reduce both heat capacity and thermal noise. The equipped adiabatic de-magnetized refrigerator (ADR) and liquid helium realize the extremely low temperature at the sensor in the vacuum dewar, whose thermal shields are cooled by Joule-Tomson coolers and two-stage Stirring coolers. The detector system is placed on the focal plane of an X-ray mirror assembly, and the 6×6 pixels realize a moderate imaging capability and unprecedented energy resolution. The Resolve telescope is emphasized with the high energy resolution of 7 eV FWHM at 6 keV. The energy resolution allows us to measure the velocity dispersion of the iron line in the accuracy of 100 km s^{-1} .

The detector assembly and the ADR cooling system are developed by NASA/GSFC, while JAXA and Sumitomo Heavy Industry (SHI) develop and provide the vacuum dewar and the mechanical cooling systems.

1.2. Xtend

The wide-field X-ray CCD imager with the identical XMA constitutes the “Xtend” telescope, which covers the same energy band of Resolve with a $200\text{ }\mu\text{m}$ thick back-illuminated CCDs.⁶ The X-ray CCD, operated at the temperature of -110°C utilizing the one-stage Stirling cooler, covers almost the same energy band from oxygen lines to highly ionized irons. The device was developed for the Hitomi/SXI and employed by XRISM with a slight modification. The CCD is produced by Hamamatsu Photonics, is calibrated by the Xtend team of XRISM, and is installed in a camera body electronics by Mitsubishi Heavy Industry (MHI).

The spacecraft of 2.3 tons is 7.9 m long, 9.2 m wide, and the baseplate diameter is about 3 m. It is designed to work for three years with cryogen of Resolve. After three years, we can conduct cryogen-free operation with installed mechanical coolers.

2. Science Cases

The high energy resolution and weak line detection capability of Resolve exceed the previous observatories above 0.8 keV. The Xtend is excellent in grasp capability, which is the product of effective area and the solid angle of field of view. With the combination of a narrow field of view, Resolve, Xtend is useful for producing reliable scientific outputs with the brand new X-ray micro-calorimeter system. The science cases with X-ray microcalorimeter are summarized in ASTRO-H White Papers.^{7–23}

2.1. *Structure formation of cluster of galaxies*

The precision of cluster cosmology depends on the accuracy of the mass measurements. One of the most important ways of measuring cluster masses is based on hydrostatic equilibrium — the assumption that the thermal pressure alone supports the hot gas against the cluster’s gravity. However, numerical simulations show that the macroscopic motions of the intra-cluster medium (ICM) may provide significant non-thermal pressure support, up to 25 – 30% at the radius at which the cluster mass density is 200 times the critical density of the universe (r_{200}).

Hitomi observed the Perseus core, which is dominated by the central massive galaxy NGC 1275, to reveal the macroscopic motion of the ICM (Fig. 1. By measuring the line doppler broadening, the Hitomi succeeded in showing that the turbulent velocity dispersion is $164 \pm 10\text{ km s}^{-1}$ as mentioned.⁴ This kinetic pressure is less than 10% of the thermal pressure on a scale of 60 kpc. XRISM will continue Hitomi’s legacy by measuring velocities of gas motions and the non-thermal pressure contribution with an accuracy of a few percent in many relaxed, bright galaxy clusters. Velocity measurements up to r_{2500} , for even a small sample of nearby relaxed clusters, will significantly improve the constraints on dark energy and other cosmological parameters.¹⁷

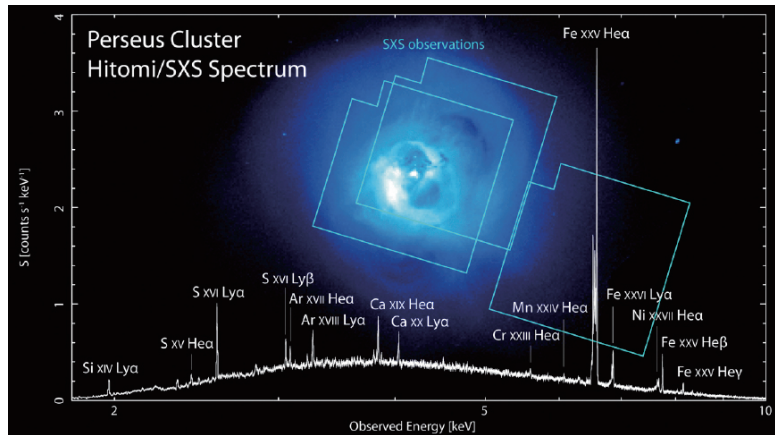


Fig. 1. Chandra image²⁴ and the Hitomi SXS spectrum from Perseus cluster of galaxies.^{4,25} The blue boxes in the image indicates the field of view of Hitmoi SXS. Hitomi observed the central region and obtained the high resolution spectrum. Evaluating the Fe-K lines width, the Hitomi collaboration⁴ reveals the turbulent velocity dispersion of $164 \pm 10 \text{ km s}^{-1}$.^a

2.2. Transportation of energy and matters

XRISM will conduct spatially and spectrally investigation on the Active Galactic Nucleus (AGN) feedback.¹⁹ Figure 2 left panel shows Chandra X-ray image of the core region of the Virgo cluster of galaxies dominated by the central galaxy M 87, which highlights the complexity of structures in the gas. We focus that the 1 keV gas indicates uplifted gas produced by the AGN feedback. These structures will be resolved by the Resolve utilizing the imaging spectroscopy capability. Each white box (6×6) shows the field of view of Resolve, and by mapping, XRISM will observe both the uplifted gas structure and surrounding ICM. Figure 2 right shows a simulated Resolve spectrum of one of the regions with the expected outflows in M 87 assuming a 100 ks exposure. The spectrum resolves the contributions from the different thermal components to the Fe-L line complex and allows us to distinguish uplifted cool gas from the ambient hot ICM.

The chemical evolution of the universe reflects the history of billions of supernovae. Resolve will detect weak lines from rare elements in the ICM, such as Na, Al, Cr, and Mn. Al and Na are sensitive tracers of the metallicity of the underlying stellar population. Also, Cr and Mn can be used to probe the characteristics of SN Ia progenitors, resulting in information about the chemical enrichment history of the ICM and the universe.

^aCredit: ISAS/JAXA <https://www.isas.jaxa.jp/feature/forefront/190924.html>.

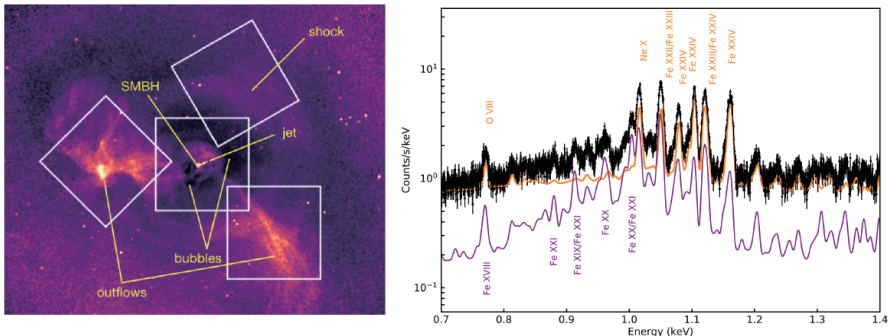


Fig. 2. Spatially and spectrally resolving AGN feedback with XRISM. Reprinted by courtesy of the authors from Figure 5 of “Science of XRISM”³⁰ which is updated from an ASTRO-H White Paper.¹⁷ **Left:** Chandra X-ray image of the core region of the Virgo cluster, including the central galaxy M 87, divided by a spherically symmetric model of surface brightness. The image highlights the complexity of structures in the gas produced by the AGN feedback.^{28,29} Each white box ($2.9' \times 2.9'$) shows the field of view of Resolve. The two regions point at the cool and bright structures, such as the shock and the center of M 87. **Right:** a 100 ks simulated Resolve spectrum of one of the regions with outflows (left box) in M 87. The spectrum shows the contributions from the different thermal components to the Fe-L line complex.

2.3. Relativistic objects

XRISM will revolutionize our understanding of accreting SMBHs, starting from how cold gas flows in from the interstellar medium (ISM) of the galaxy down to the inner accretion flow where matter is affected by the strong gravity of the black hole.¹⁸

Relativistic Doppler broadening and gravitational redshifts in the accretion disks surrounding black holes have been investigated for decades.²⁶ In particular, the ASCA observation of MCG-6-30-15 opened our observational view of a broad Fe K line in AGN X-ray spectra.²⁷ The implication of the broad line is immense, as it may provide a way of measuring an elusive fundamental parameter of a black hole — spin. As such, the broad Fe-K line has ignited debate and continued interest.

Rapid time variability shown in the following observations, including the X-ray reverberation mapping or quasar microlensing, improved our understandings. They indicate that the broad Fe K line is produced by reprocessing the inner accretion disk within $\sim 10R_g$. However, the details of the inner disk radius and kinematics of the flow are still highly debated.

By disentangling the expected contributions from other spectral features — narrow emission from the outer disk and torus or absorption through ionized outflows along our line of sight —, XRISM probes properties of the inner accretion flow to estimate the black hole spin. Thus, we will clearly understand how much material is making it to the black hole and how much material is removed through massive outflows.

Figure 3 left chart shows Fe-K line profile of MCG-6-30-15 as seen in 300 ks by XMM-Newton pn (blue) and Chandra HETGS (green), along with a Resolve simulation in red. The red XRISM spectrum alone shows clear spectral features in this Fe-K energy band. The middle chart shows The ratio of the XMM pn spectrum to a power-law model t between 2 and 4 keV, and 7.5 and 10 keV. The pn spectrum can be well described either by pure relativistic reflection with an inclination of 5 deg (blue) or by relativistic reflection with an inclination of 75 deg with additional emission and absorption, including an ultrafast outflow of $v_{\text{out}} = 0.13 c$ (red). The right panel shows that XRISM will easily distinguish between these two scenarios since it resolves the narrow emission and absorption features.

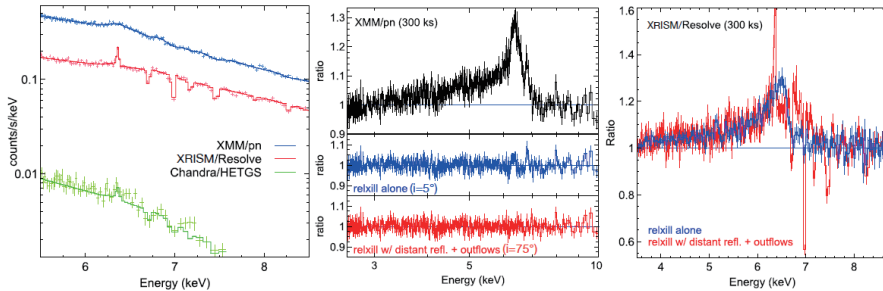


Fig. 3. Reprinted by courtesy of the authors from Figure 6 of “Science of XRISM.” **Left:** Fe-K line profile of MCG-6-30-15 as seen in 300 ks by XMM-Newton pn (blue) and Chandra HETGS (green), along with a Resolve simulation in red. **Middle:** The ratio of the XMM pn spectrum to a power-law model fit between 2–4 keV and 7.5 – 10 keV. The pn spectrum can be equally well described by pure relativistic reflection with an inclination of 5 deg (shown in blue) or by relativistic reflection with an inclination of 75 deg with additional emission and absorption, including an ultrafast outflow of $v_{\text{out}} \sim 0.13 c$ (shown in red). **Right:** XRISM will easily distinguish between these two scenarios, as the narrow emission and absorption will be resolved.³⁰

The relativistic redshift on a compact object surface is also one of the scientific targets of XRISM. Here we show an example of the symbiotic star detected by Swift/BAT T Coronae Borealis (T CrB), which is a recurrent nova.⁹ This fact and the hard BAT spectrum indicate that its white dwarf is exceptionally massive, around 1.35 solar mass.

T CrB exhibits a strong 6.4 keV Fe-K line, partly from the reflection of the white dwarf surface. Therefore, T CrB is an ideal target to investigate the compact object’s mass and radius by measuring the gravitational redshift. This simulated spectrum is guided using the 46 ks Suzaku observation obtained in 2006.³¹ The XIS data were reproduced well with a model absorbed by a partial covering absorber, with a single, narrow Gaussian at 6.396 keV. If it is, the inset shows that the XRISM Resolve has the statistical quality necessary to detect the expected gravitational redshift of 4 eV of the neutral iron-K line (Fig. 4).

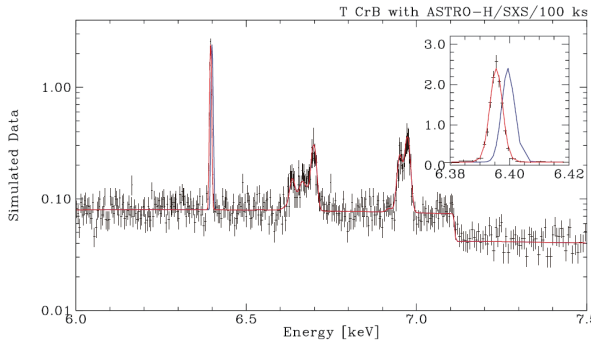


Fig. 4. Simulated 100 ks observation of T CrB in the Fe-K α region. The inset showing a close-up spectrum around the energy of 6.4 keV. It shows the Resolve has a capability to detect the expected gravitational redshift of 4 eV (see text). Reprinted by courtesy of the authors from Figure 2 of “ASTRO-H White Paper – White Dwarf”⁹

3. Mission Status and Observation Plan

All the instruments produced under the international collaboration are being delivered to the JAXA Tsukuba Space Center. The Resolve calorimeter sensor insert was delivered and installed in the dewar produced in SHI, Japan. The integrated dewar system equipped with the mechanical coolers was transferred to Tsukuba Space Center with the cooler drivers. The XMA is under calibration and is planned to be delivered to Japan in January 2022. All CCD chips for the Xtend were screened in Osaka University and were integrated into the camera system at MHI. The camera was transferred to Tsukuba Space Center. In 2022, these mission instruments will be installed on the satellite in the first half. Then we conduct the proto-flight test. XRISM will be launched in the Japanese Fiscal Year 2022 or the early calendar year 2023 from Tanegashima Space Center.

Table 2. XRISM observation phases

Initial phase	3 months
critical operation commissioning	~ 1 week until 3 months after launch
Nominal phase	until 3 years after launch
initial calibration & test observations	1 month
calibration & performance verification observation	6 months
nominal observation (Guest observations)	26 months

Observation phases defined in the operation plan are summarized in Table 2. At the beginning of the nominal observation phase, the performance verification (PV)

observations are conducted. The initial observation phase is planned to verify the performance to show the XRISM capability to the astrophysics community. The PV observation target objects list was recently released on the XRISM website for researchers.^b The XRISM Science Team consists of contributors to develop instruments, data processing software, and calibration and observation plan to carry out the PV observations. In addition to the XRISM Science Team, unlike Hitomi, XRISM introduced the XRISM Guest Scientist Program to the PV phase observation. The XGSs will be solicited by the three agencies — JAXA, NASA, and ESA independently — in 2022 and contribute to PV observation planning, data analysis, and produce science output with the XRISM Science Team. The guest observer phase is open 10 months after the launch. The announcement of opportunity for the guest observations is planned to be submitted at the end of the commissioning.

The approved nominal mission term is 3 years. After the 3 years, the XRISM project is to have a mission completion review. At the moment, if the satellite, including the mechanical cooling system, functions well and the mission extension review approve, the latter phase operation will be conducted in the latter half of the 2020s.

Acknowledgments

XRISM is a JAXA mission joint with NASA in collaboration with ESA. The XRISM Science Team studies the science cases described in this paper based on the previous research by the ASTRO-H Science Working Group.

References

1. M. S. Tashiro et al, Concept of X-ray Astronomy Recovery Mission (XARM), in *Proc. SPIE: Space Telescopes and Instrumentations 2018: Ultraviolet and Gamma-Ray*, **10699** eds. J-W. A. den Herder, S. Nikzad, (2018) id. 1069922.
2. M. S. Tashiro et al, Status of X-ray Imaging and Spectroscopy Mission (XRISM), in *Proc. SPIE: Space Telescopes and Instrumentations 2020: Ultraviolet and Gamma-Ray*, **11444** eds. J-W. A. den Herder, S. Nikzad, K. Nakazawa (2020) id. 1144422.
3. T. Takahashi et al., *Journal of Astronomical Telescopes, Instruments, and Systems*, **4** (2018) id. 021402.
4. Hitomi Collaboration, *Nature*, **535** (2016) 117.
5. Y. Ishisaki et al., Status of resolve instrument for X-ray imaging telescope (Xtend) onboard X-ray Astronomy Recovery Mission (XARM), in *Proc. SPIE: Space Telescopes and Instrumentations 2018: Ultraviolet and Gamma-Ray*, **10699** eds. J-W. A. den Herder, S. Nikzad, (2018) id. 1069924.
6. K. Hayashida et al, Soft X-ray imaging telescope (Xtend) onboard X-ray Astronomy Recovery Mission (XARM), in *Proc. SPIE: Space Telescopes and Instrumentations 2018: Ultraviolet and Gamma-Ray*, **10699** eds. J-W. A. den Herder, S. Nikzad, (2018) id. 1069923.

^b<https://xrism.isas.jaxa.jp/research/>

7. T. Takahashi et al., ASTRO-H Space X-ray Observatory White Paper, *arXiv*, (2014) 1412.2351.
8. Y. Tsuboi et al., ASTRO-H Space X-ray Observatory White Paper - Stars – Accretion, Shocks, Charge Exchange and Magnetic Phenomena, *arXiv*, (2014) 1412.1162.
9. K. Mukai et al., ASTRO-H Space X-ray Observatory White Paper - White Dwarf, *arXiv*, (2014) 1412.1163.
10. C. Done et al., ASTRO-H Space X-ray Observatory White Paper - Low-mass X-ray Binaries, *arXiv*, (2014) 1412.1164.
11. S. Kitamoto et al., ASTRO-H Space X-ray Observatory White Paper - Accreting Pulsars and Related Sources, *arXiv*, (2014) 1412.1165.
12. J. Miller et al., ASTRO-H Space X-ray Observatory White Paper - Stellar-Mass Black Holes, *arXiv*, (2014) 1412.1173.
13. J. P. Hughes et al., ASTRO-H Space X-ray Observatory White Paper - Young Supernova Remnants, *arXiv*, (2014) 1412.1169.
14. K. S. Long et al., ASTRO-H Space X-ray Observatory White Paper - Old Supernova Remnants and Pulsar Wind Nebulae, *arXiv*, (2014) 1412.1166.
15. K. Koyama et al., ASTRO-H Space X-ray Observatory White Paper - Plasma Diagnostic and Dynamics of the Galactic Center Region, *arXiv*, (2014) 1412.1170.
16. F. Paerels et al., ASTRO-H Space X-ray Observatory White Paper - High Resolution Spectroscopy of Interstellar and Circumgalactic Gas in the Milky Way and Other Galaxies, *arXiv*, (2014) 1412.1174.
17. T. Kitayama et al., ASTRO-H Space X-ray Observatory White Paper - Clusters of Galaxies and Related Sources, *arXiv*, (2014) 1412.1176.
18. C. Reynolds et al., ASTRO-H Space X-ray Observatory White Paper - AGN Reflection, *arXiv*, (2014) 1412.1177.
19. J. S. Kaastra et al., ASTRO-H Space X-ray Observatory White Paper - AGN Reflection, *arXiv*, (2014) 1412.1171.
20. R. K. Smith et al., ASTRO-H Space X-ray Observatory White Paper - New Spectral Features, *arXiv*, (2014) 1412.1172.
21. F. Aharonian et al., ASTRO-H Space X-ray Observatory White Paper - Shock and Acceleration, *arXiv*, (2014) 1412.1175.
22. P. Coppi et al., ASTRO-H Space X-ray Observatory White Paper - Broad-band Spectroscopy and Polarimetry, *arXiv*, (2014) 1412.1190.
23. M. S. Tashiro et al., ASTRO-H Space X-ray Observatory White Paper - Chemical Evolution in High-z Universe, *arXiv*, (2014) 1412.1179.
24. I. Zhuravleva, et al., NASA/CXC/Stanford.
25. Hitomi Collaboration, *Nature*, **551** (2017) 478.
26. A. C Fabian, et al., *MNRAS* **238** (1989) 729.
27. Y. Tanaka et al., *Nature* **6533** (1995) 659.
28. W. Forman et al., *ApJ*, **665** (2007) 1057.
29. A. Simionescu et al., *A&A* **482** (2008) 97.
30. XRISM Science Team, Science with the X-ray Imaging and Spectroscopy Mission (XRISM), *arXiv*, (2020) 2003.04962.
31. G. J. M. Luna et al., RS Ophiuchi (2006) and the Recurrent Nova Phenomenon ASP Conference Series, **401** (2007) 342.